

# The Mass-Luminosity Relation in AGN

A. Wandel

*Racah Institute, The Hebrew University, Jerusalem 91904, Israel*

**Abstract.** Probably the most fundamental characteristic of the quasar-AGN power house, the mass of the central black hole, is the least well known. The broad emission lines have been, and probably will remain, our best probe of the central mass. Using these probes to estimate the black hole mass suggests that over more than six orders of magnitude, the ratio between the continuum luminosity and the central mass (the Eddington ratio) has a spread perhaps as narrow as 1–2 orders of magnitude, while other methods give a larger spread and possibly a luminosity-dependent Eddington ratio. I review the three main classes of mass estimation methods—BLR kinematics, X-ray variability and accretion disk modeling, and their results for  $L/L_{\text{Edd}}$ . Potential sources of error and biases are discussed.

## 1. The $L/M$ relation and mass estimation methods

The most fundamental, yet the least well known, parameter of the AGN central engine is its mass. While the AGN luminosity, which is readily measurable, varies over six orders of magnitude, the ratio  $L/M$  (or, alternatively, the Eddington ratio,  $L/L_E$ ) apparently has a rather small range, indicating that the  $L/M$  value is a property characterizing the AGN phenomenon. In terms of the Eddington ratio we find from various mass estimation methods and for various AGN samples  $L/L_E \sim 0.001\text{--}1$ . This value and its spread depend on the method used to estimate the mass.

The methods used to determine the central mass in AGN can be divided into three major groups: BLR kinematics, X-ray variability and accretion disk spectral fitting. The first group uses the broad emission lines as probes, assuming the velocity dispersion of the line-emitting gas is induced by the gravitational potential of the central mass. The second gives the variability mass limit (eq. 1), while the third is a variant of the temperature mass (eq. 2), essentially trying to fit the UV bump with a spectrum from a thin accretion disk model. In the following sections I will describe the three groups and the problems associated with each of them.

## 2. Some fiducial masses

Any compact, accretion-powered radiation source can be assigned several fiducial mass estimates:

1. The Eddington limit. In order to maintain steady spherical accretion the luminosity must be less than the Eddington luminosity,  $L < L_{\text{Edd}} = 4\pi GMm_p c/\sigma_T = 1.3 \times 10^{46} M_8 \text{ erg s}^{-1}$ , or  $M_8 > L_{46}$  where  $M_8 = M/10^8 M_\odot$  and  $L_{46} = L/10^{46} \text{ erg s}^{-1}$ .

2. The variability limit. The shortest time scale for global variations in the luminosity is the light travel time across the Schwarzschild radius,  $R_s/c = 2GM/c^3 = 10^3 M_8 \text{ s}$ . Hence if the luminosity is observed to vary significantly on a time scale  $\Delta t$ , the black hole mass has to be

$$M_8 < (\Delta t/10^3 r^{-1} \text{ s}), \quad (1)$$

where  $r$  is the effective radius of emission in units of  $R_s$ .

3. The temperature mass. If a luminosity  $L$  comes from an accretion disk region of radius  $R$  and temperature  $T$ , then  $L < 4\pi R^2 \sigma T^4$ . If a spectral feature at frequency  $\nu$  is due to emission from a black body accretion disk at a characteristic radius  $R$ , then the temperature is given by  $h\nu = 3kT$ , and we have an upper limit on the black hole mass:

$$M_8 > 100(T/10^5 \text{ K})^{-2} L_{46}^{1/2} (R/R_s)^{-1}. \quad (2)$$

4. The evolutionary mass. This mass involves the evolution of a massive black hole due to accretion. We may define the Eddington time  $t_E$  as the time required for an accretion-powered object radiating at the Eddington luminosity to double its mass,  $t_E = Mc^2/L_E = 4 \times 10^8 \text{ y}$ . The observed luminosity implies an accretion rate of  $\dot{M} = 0.16\epsilon^{-1} L_{46} M_\odot \text{ y}^{-1}$  where  $\epsilon$  is the efficiency. Combining these two expressions gives the evolutionary mass, accumulated if the accretion rate is maintained during a time  $t_E$  :

$$M_8 = 0.6\epsilon^{-1} \eta^{-1} f_L L_{46} \quad (3)$$

where the parameters  $\eta$  and  $f_L$  are the Eddington luminosity ratio and the fraction of the active time for intermittently active AGN.

### 3. BLR kinematics

The broad emission lines characteristic of quasar and Seyfert 1 spectra are believed to originate from gas highly ionized by the continuum radiation of the central source. The line width must be due to bulk motions, probably an ensemble of clouds moving in the gravitational potential of the central black hole . Alternative scenarios include radiative acceleration (e.g. Blumenthal and Mathews 1975), which would induce radial outflow. However, radial motions are probably excluded because they would induce asymmetric line profiles (if the emitting clouds are optically thick) which are usually not observed. Most workers today agree that the line width in AGN is induced by Keplerian bulk motions. If this is the case, knowledge of the distance of the line-emitting gas from the central mass would allow us to estimate the black hole mass,

$$M \approx v^2 R/G. \quad (4)$$

The kinematic mass-estimation methods can be divided into two sub-groups, depending on the method used to find the emission-line distance: photoionization methods and reverberation mapping.

### 3.1. Photoionization: the ionization-parameter method

We assume that the spatial extent of the BLR may be represented by a characteristic size — e.g. the radius at which the emission peaks. Indeed, reverberation analyses have shown that the time lag of emission-line variability varies depending on the line, and the emission region may be extended in radius. However, photo-ionization calculations have shown that the line emissivities of many lines peak sharply in a relatively narrow range of density and ionization parameter (Baldwin et al. 1995). Depending on the radial variation of the density this may imply that the emission of a given line is localized in a relatively narrow shell around the continuum source. Given these results, the single radius model may be a reasonable approximation for a particular emission line. The physical conditions in the line-emitting gas are largely determined by the ionization parameter (the ratio of ionizing photon density to the electron density,  $n_e$ , e.g. Netzer 1990)  $U = Q_{ion}/4\pi r^2 c n_e$  where the ionizing photon flux (number of ionizing photons per unit time) is  $Q_{ion} = \int_{E_0}^{\infty} F(E) \frac{dE}{E}$ .  $F(E)$  is the luminosity per unit energy, and  $E_0$  is the ionization potential of the line under consideration (1 Rydberg=13.6 eV for the hydrogen lines). Defining the ionizing luminosity,  $L_{ion} = \int_{E_0}^{\infty} F(E) dE$  and the mean energy of an ionizing photon,  $\bar{E}_{ion} \equiv L_{ion}/Q_{ion}$ , the BLR radius may be written as

$$r = \left( \frac{L_{ion}}{4\pi c \bar{E}_{ion} U n_e} \right)^{1/2} = 13.4 \left( \frac{L_{44}}{U n_{10} \epsilon} \right)^{1/2} \text{ light-days} \quad (5)$$

where  $n_{10} = n_e/10^{10} \text{ cm}^{-3}$ ,  $L_{44} = L_{ion}/10^{44} \text{ erg s}^{-1}$ , and  $\epsilon = \bar{E}_{ion}/E_0$  is the mean photon energy in units of  $E_0$ . Combining equations 4 and 5 we get the expression for the black hole mass (in units of  $10^8 M_{\odot}$ ):

$$M_8 = 0.5 v_3^2 \left( \frac{L_{44}}{U n_{10} \epsilon} \right)^{1/2} \quad (6)$$

where  $v_3 = v(FWHM)/10^3 \text{ km s}^{-1}$ . Analyses of the broad emission lines in various AGN indicate that typical values in the gas emitting the high excitation broad lines are  $U \sim 0.1\text{--}1$  and  $n_e \sim 10^{10}\text{--}10^{11} \text{ cm}^{-3}$  (e.g. Rees, Netzer & Ferland, 1989), so that  $U n_{10} \sim 0.1\text{--}10$ . For a given ionizing spectrum, one can explicitly calculate the photon flux  $Q_{ion}$ , or alternatively  $\epsilon$  and  $L_{ion}$  in eq. 5. The ionizing flux is dominated by the EUV continuum in the 1–10 Rydberg regime, where most of the ionizing photons are emitted. Since the continuum in this range cannot be observed directly, it may be estimated by extrapolation from the nearest observable energy bands: the UV and soft X-rays. The far UV spectrum has been observed beyond the Lyman limit for about 100 quasars to wavelengths of 600 Å (Zheng et al. 1996). Wandel (1997) uses an estimate of the ionizing flux based on the soft X-ray continuum spectrum. This approach is particularly appropriate for lines with high ionization potentials such as C IV and O VI, which are derived from more energetic photons, thus closer to the soft X-ray band.

### 3.2. The emission-volume method

A different approach that does not require the thin shell assumption tries to estimate the size of the emitting volume. Assuming this volume to be roughly

spherical, the line luminosity would be (Dibai 1981)

$$L_{line} = \frac{4\pi}{3} R^3 f_v j_{line}, \quad (7)$$

where  $j_{line}$  is the line volume emissivity and  $f_v$  is the volume filling factor. Dibai (1981) took  $f_v = 0.001$  which is arbitrary and probably an overestimate. Wandel & Yahil (1985) elaborated the method by expressing  $f_v$  in terms of the better known  $f_a$ , the angular covering factor:  $f_v \approx \frac{f_a N}{nR}$ , where  $N$  is the column density of the line emitting gas. Substituting this into equation 7 gives (for the H $\beta$  line)

$$R = 15 \left( \frac{L(H\beta)}{10^{42} \text{ erg s}^{-1}} \right)^{1/2} (n_{10} N_{23} \frac{f_a}{0.1})^{-1/2} \text{ light-days}, \quad (8)$$

where  $N_{23} = N/10^{23} \text{ cm}^{-2}$ . The implied kinematic black hole mass is obtained by combining this with eq. 4,

$$M_8 = 0.4 v_3^2 \left( \frac{L_{42}(H\beta)}{n_{10} N_{23} f_a / 0.1} \right)^{1/2}. \quad (9)$$

Applying this method for a sample of about 90 low-redshift AGN (mainly Seyfert 1 galaxies and quasars), Wandel & Yahil (1985) found a tight correlation between the black hole mass (inferred from the H $\beta$  line) and the absolute magnitude (fig. 1). A similar value may be obtained from the sample of Joly et al. (1985).

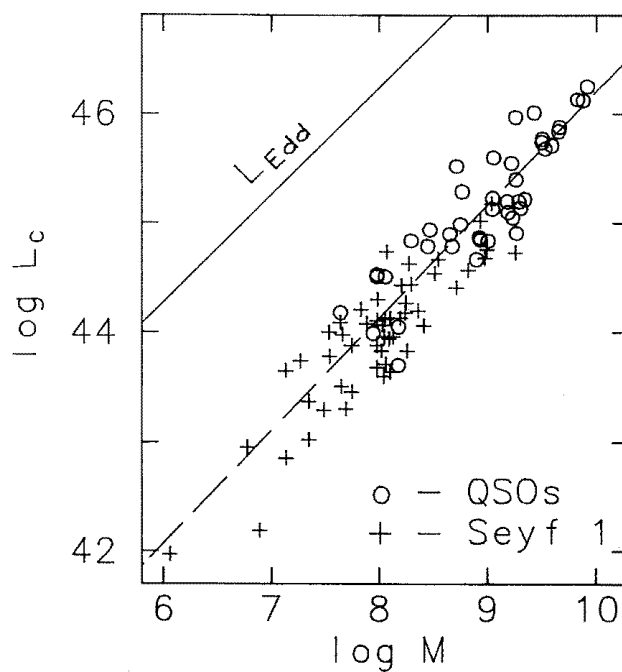


Figure 1. Optical luminosity versus the mass calculated with the emission volume method from the H $\beta$  line.

Although in part this correlation is expected, because of the known strong correlation between the line and continuum luminosities, the correlation found is actually steeper and stronger than the expected one. If true, this correlation may imply a universal mass-luminosity relation, which, in terms of the Eddington luminosity ( $L_{\text{Edd}} = 1.3 \times 10^{45} M_8 \text{ erg s}^{-1}$ ), can be expressed as  $\log L/L_{\text{Edd}} = -2 \pm 0.5$ .

### 3.3. The narrow emission lines

Similar methods can be applied to the narrow emission-line region (NLR), provided the gas there is gravitationally bound. Typical parameter values for the NLR are  $Un_{10} = 10^{-10}$  and  $f_a = 0.01$  (e.g. Brotherton et al. 1994). Of course, within the distance of the NLR from the center, the stellar mass of the host galaxy could be comparable to the mass of the central black hole, but they may be correlated (see Laor 1998). Wandel & Mushotzky (1986) find an excellent correlation between the mass estimated from the narrow-line width and the black hole mass estimated from X-ray variability (fig. 3 in section 4 below). Wandel & Mushotzky (1986) also apply this method to a sample of Seyfert 2 galaxies finding that Seyfert 2s as a group obey the same correlation, provided we observe only a fraction (0.1) of the emitted X-ray continuum. This is consistent with presence of an obscuring torus, as suggested by the unified scheme of AGN.

### 3.4. Reverberation mapping

Variability in the continuum UV luminosity is observed to be followed by corresponding changes in the line luminosity with delays ranging from days in low-luminosity AGN to months in luminous quasars. Cross-correlating the continuum and emission-line light curves gives the peak of the power in the delay and the characteristic size ( $R_\tau = c\tau$ ) of the emission-line region. Using this size in eq. 4 gives an alternative method to calculate the black hole mass. Combining all the objects with reliable reverberation data, it appears that  $R \propto L^{1/2}$  (Peterson 1994; Kaspi 1997). With this dependence in mind, eq. 4 gives a similar empirical dependence to that in eqs. 6 and 9:  $M \propto v^2 L^{1/2}$ . The effective BLR radii for the reverberation and ionization-parameter methods (both for the H $\beta$  line) have been found to agree very well, particularly when the shape of the ionizing continuum is taken into account (Wandel 1997). So do of course the inferred masses.

### 3.5. The variable component of the line profile: RMS spectrum

Although giving a more direct measurement of the BLR size than the photoionization methods, the reverberation mapping kinematic method has two drawbacks:

- Very few AGN (about a dozen) have reliable reverberation data. Measuring the reverberation radius requires many observations and is a large project.
- It is not clear that the line variability size measured by the technique of reverberation (or echo) mapping is the same one contributing the emission-line profile.

The line profile is given by

$$f(\Delta\lambda) = 4\pi \int_{R_{in}}^{R_{out}} \delta[v(R) \sin(i) - c(\Delta\lambda/\lambda)] E(R) R^2 dR \quad (10)$$

where  $E(R)$  is the volume line emissivity at a radius  $R$  and  $i$  is the inclination angle to the line of sight. This may be used to define a velocity-weighted radius, e.g.  $R_{FWHM}$ , associated with the FWHM of the line profile. A related radius is the emissivity-weighted radius, that may be defined by

$$R_{em} = \int_{R_{in}}^{R_{out}} E(R) R^3 dR / \int_{R_{in}}^{R_{out}} E(R) R^2 dR. \quad (11)$$

The reverberation radius is obtained by cross correlating the line and continuum light curves.

For a thick geometry these radii may be quite different. One solution to this difference is to combine the reverberation-mapping radius with the velocity inferred from the variable component of the line profile. In this method, the distance of the line-emitting gas from the central source (the reverberation radius) and its velocity dispersion (given by the rms spectrum, which reflects only the variable part of the emission-line profile) both refer to the same gas. Comparing the rms reverberation and the ionization-parameter methods, one may calibrate the latter, which is easier to use and may be applied also for objects without variability data.

### 3.6. Uncertainties and potential error sources

There are several drawbacks which introduce possible errors into the emission-line kinematic methods:

- Uncertainty and scatter in the parameters. In the ionization method we do not know the values of  $n$  and  $U$ .
- In the volume-emission method the parameters  $N$ ,  $f_a$  and  $n$  are uncertain.
- The velocity of the emitting gas may be anisotropic.
- The illumination of the clouds may be anisotropic.
- The motions may be due to non-gravitational forces.

## 4. Time variability

The AGN continuum is known to vary on time scales that depend on the wavelength and luminosity. While for the UV the time scale ranges from days to months (depending on the luminosity), the time scale for variations in X-rays is of the order of hours. As we have seen above, the variability can be used to place a lower limit on the black hole mass. If we knew the radial dependence of the local X-ray spectrum in the inner disk, the effective emission radius in eq. 2 would be

$$R_{eff} = \int_{R_{in}}^{R_{out}} F_x(R) R^2 dR / \int_{R_{in}}^{R_{out}} F_x(R) R dR \quad (12)$$

where  $F_x(R)$  is the X-ray emissivity per unit area from the disk at radius  $R$ . Since there is no widely accepted model for the X-ray continuum emission in AGN, we assume  $R_{eff}$  is a few Schwarzschild radii, e.g.  $5R_s$ , where the emission from the thin disk around a Schwarzschild black hole peaks. For this value eq. 1 gives  $M_8 < 0.5\Delta t/10^4$  s. Barr & Mushotzky (1986; fig. 2) have found a good correlation between  $\Delta t$  and the X-ray luminosity.

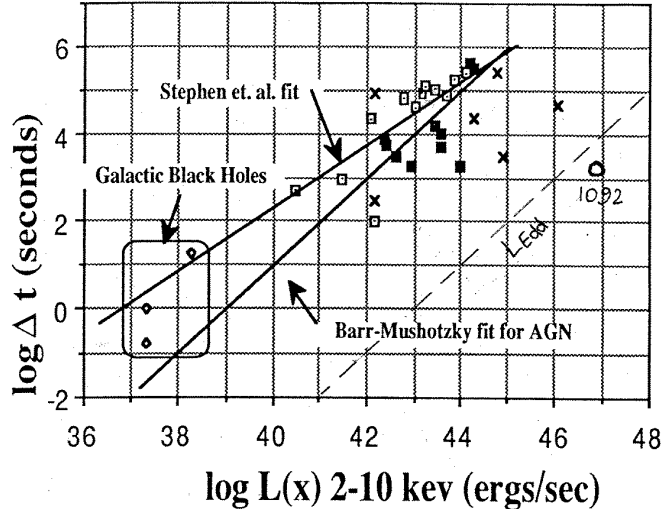


Figure 2. X-ray variability time scale versus X-ray luminosity. Circles — Barr & Mushotzky (1986), squares — EXOSAT data, crosses — radio-bright objects. Solid lines are best fits (with and without Galactic black holes). The dashed line indicates the Eddington limit assuming  $R = 5R_s$ .

While the variability masses of quasars and Seyfert 1s seem to give Eddington ratios well below unity, some bright radio objects (e.g. BL Lacs) as well as some Narrow-Line Seyfert 1 galaxies (NLS1) have values close to unity and even larger than unity, e.g. PHL 1092 (see Brandt & Boller 1998). Taking into account the data on Galactic black holes and bright radio sources, one gets a smaller slope in the  $L$ - $\Delta t$  plane, which may be interpreted (assuming  $M \propto \Delta t$ ) as the  $L/M$  ratio increasing with luminosity. It may therefore be of interest to compare the masses derived by the variability method (which admittedly gives only an upper limit) with the predictions of other methods, in order to find how tight the upper limits are, or how well they correlate with the real mass. Wandel & Mushotzky (1986) find a very good linear correlation between the X-ray variability time and the kinematic mass (calculated from the [O III] line; see fig. 3), which supports the hypothesis that  $\Delta t$  (X-ray) and the FWHM of [O III] both are closely related to the central mass. Interestingly, in the sample used by Wandel & Mushotzky (1986), the correlation of  $\Delta t$  with the mass derived from H $\beta$  is less good than that with the mass derived from [O III]. For broad lines, a good correlation between  $\Delta t$  (X-ray) and the H $\beta$  line width is obtained in a

mixed sample containing rapidly variable NLS1 and normal Seyfert 1s (Wandel & Boller 1998).

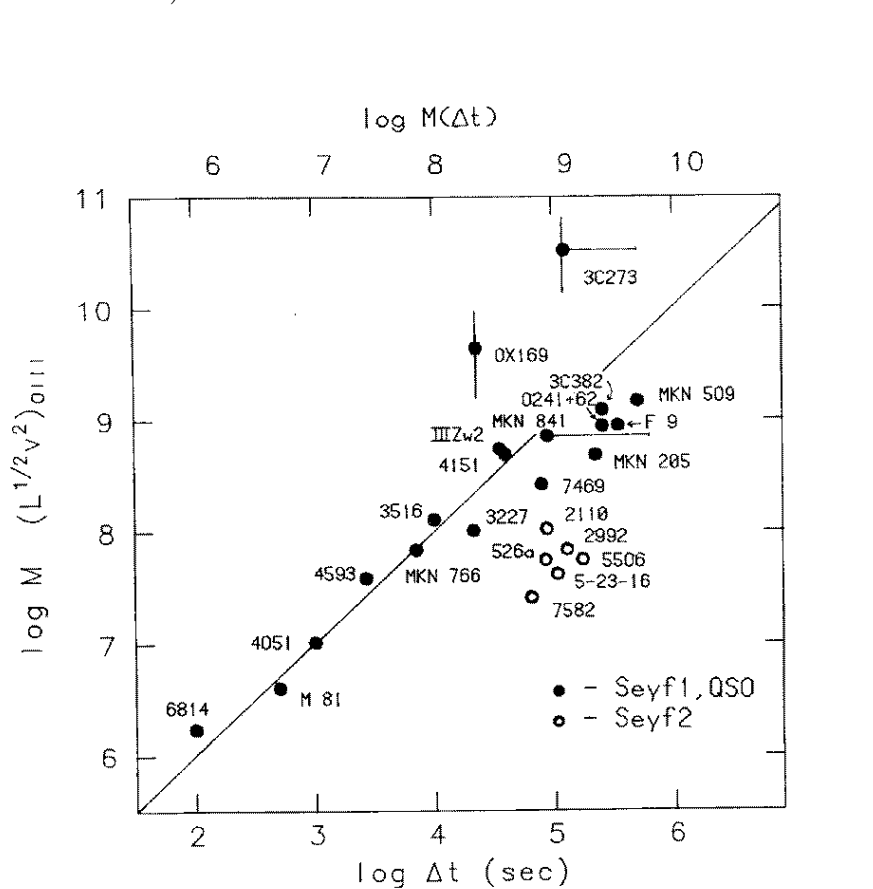


Figure 3. X-ray variability time versus [O III] kinematic mass estimate (Wandel and Mushotzky 1986).

## 5. Accretion-disk modeling

Many authors have tried to fit accretion disk spectra to the observed AGN continuum, thus finding the accretion disk parameters ( $M, \dot{M}, \alpha$  and the angular momentum of the black hole) which best fit the observed continuum in the UV (e.g. Wandel & Petrosian 1988; Sun & Malkan 1991) or in the soft X-rays (e.g. Laor 1990).

### 5.1. The accretion disk - black body spectral relation

The thin accretion disk spectrum is a multi-temperature black body one, and trying to fit the UV bump (or the soft X-ray spectrum) is essentially equivalent to using eq. 2 in order to find the temperature-mass:  $M_8 \approx 3L_{45}^{1/2}/T_5^2(r/10)$

where  $r = R/R_s$ . The second accretion disk parameter,  $\dot{M}$ , is determined by the observed luminosity, schematically via the relation  $L = \epsilon Mc^2$ . An alternative approach relates the peak in the accretion disk spectrum to the thin accretion disk parameters by assuming the spectrum is dominated by black body emission near the maximum-surface emissivity radius. This gives

$$E_{max} \approx 3kT_{bb}(5R_s) = 10(\dot{m}/M_8)^{1/4} \text{ eV} \quad (13)$$

where  $\dot{m} = \dot{M}/\dot{M}_{Edd}$  is the Eddington ratio. More sophisticated approaches, like taking as  $T_{max}$  the temperature at the inner boundary between the black body and the radiation-dominated disk or the temperature at which the inner disk becomes optically thin give  $E_{max} \approx 2(\dot{m}M_8)^{-0.3}$  eV. While in the UV band the thin accretion disk multiple black body spectrum may be a good approximation, the soft X-rays may be produced by a hotter medium due to processes other than black body emission, such as Comptonization, a two-temperature disk (Wandel & Liang 1991) or hot corona (Haardt & Maraschi 1993; Czerny, Witt & Zycki 1996).

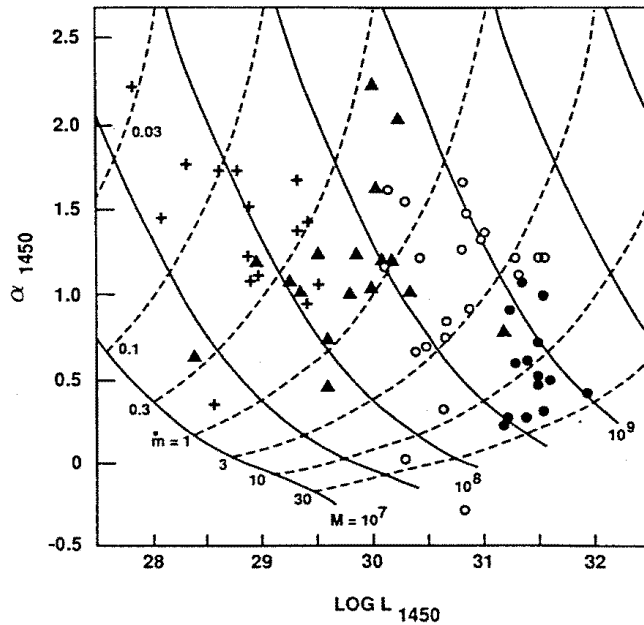


Figure 4. Accretion-disk black hole evolution tracks in the  $\alpha - L$  plane (Wandel & Petrosian 1988). Crosses: Seyfert galaxies, triangles, open circles and filled circles: low, medium and high redshift quasars, respectively. Continuous lines: constant mass; dashed lines: constant  $\dot{M}/M$  (note that, unlike in the text, the labeling of the curves in the figure follows the notation  $\dot{m} = 16.7\dot{M}/\dot{M}_{Edd}$ ).

## 5.2. Deriving $M$ and $\dot{M}$ from the UV spectrum

It is possible to perform a more refined treatment, calculating for each pair of accretion disk parameters  $M$  and  $\dot{M}$  not the total luminosity and blue-bump

temperature, but the actual observables, e.g. the UV luminosity and spectral index. Wandel & Petrosian (1988) have calculated the accretion disk flux and spectral index at 1450 Å for a grid of accretion disk parameters ( $M, \dot{M}$ ). Inverting the grid they have obtained contours of constant black hole mass and constant Eddington ratio ( $\dot{m}$ ) in the  $L - \alpha_{UV}$  plane (fig 4). Plotting in this plane samples of AGN it is possible to read from the contours the corresponding accretion disk parameters. Comparing several groups of AGN a systematic trend appears: higher redshift and more luminous objects tend to have larger black hole masses and luminosities closer to the Eddington limit (see table 1). Similar results are obtained by Sun & Malkan (1991).

Table 1. Grouping of AGN accretion disk parameters.

AGN group	$\log F_{1450}$	$\log M/M_{\odot}$	$\dot{M}/\dot{M}_{\text{Edd}}$
Seyfert galaxies	28–29.5	7.5–8.5	0.01–0.5
Low $z$ quasars	29–30.5	8–9	0.02–0.1
Medium $z$ quasars	30–31.5	8–9.5	0.1–0.5
High $z$ quasars	31–32	9–9.5	0.03–2

Table 2.  $L/M$  ratios found by various methods.

Method	$L/L_{\text{Edd}}$	Reference
<b>Kinematic</b>		
Emission Volume ( $\text{H}\beta$ )	0.003–0.03	Wandel & Yahil (1995)
Ionization parameter ( $\text{H}\beta$ )	0.01–0.1	Joly et al. (1995)
IP + Reverberation( $\text{H}\beta$ )	0.01–1	Wandel (1997)
<b>X-ray variability</b>		
X-rays	0.003–0.1	Barr & Mushotzky (1986)
X-rays+OIII photoionization	0.003–0.1	Wandel & Mushotzky (1986)
Soft X-rays, NLS1	0.001–0.1	Wandel & Boller (1998)
<b>Accretion-disk fitting</b>		
Modified BB disk	0.001–2	Wandel & Petrosian (1986)
Kerr black hole disk	0.01–2	Sun & Malkan (1991)
GR effects	0.003–0.3	Laor (1990), Laor (1993)
Disk+Corona	0.001–0.3	Czerny, Witt & Zycki (1996)

## 6. Summary

The  $L/M$  ratios found by various methods are summarized in table 2. All emission-line kinematic methods give a relatively narrow  $L/M$  range over a large range in luminosity, suggesting a universal  $L/M$  relation in AGN. However, this may be related to the fact that the samples with available data are mostly low redshift, relatively low-luminosity objects. The two other methods — X-ray variability and accretion disk fitting of the UV bump — suggest a trend of the Eddington ratio increasing with luminosity.

## References

Baldwin, J.A. et al. 1995, *ApJ*, 455, L118  
Barr, P. & Mushotzky, R.F. 1986, *Nature*, 320, 421  
Blumenthal, G.B. & Mathews, W.G. 1975, *ApJ*, 198, 517  
Brandt, W.N. & Boller, Th. 1998, in *Structure and Kinematics of Quasar Broad Line Regions*, ed. Gaskell, C.M., Brandt, W.N., Dietrich, M., Dultzin-Hacyan, D. & Eracleous, M. (ASP Press: San Francisco), p. 000  
Brotherton, M.S. et al. 1994, *ApJ*, 430, 495  
Czerny, B., Witt, H.J. & Zycki, P.T. 1996, *astro-ph/9609180*  
Dibai, E.A. 1981, *Soviet Astronomy Letters*, 7, 248  
Haardt, F. & Maraschi, L. 1993, *ApJ*, 413, 507  
Joly, M., Collin-Souffrin, S., Masnou, J.L. & Nottale, L. 1985, *A&A*, 152, 282  
Kaspi, S. 1997, in *Astronomical Time Sequences*, ed. Maoz, D. et al. (Kluwer: Dordrecht), p. 243  
Laor, A. 1990, *MNRAS*, 246, 369  
Laor A. 1998, in *Structure and Kinematics of Quasar Broad Line Regions*, ed. Gaskell, C. M., Brandt, W. N., Dietrich, M., Dultzin-Hacyan, D. & Eracleous, M. (ASP Press: San Francisco), p. 000  
Mathews, W.G. & Ferland, G.J. 1987, *ApJ*, 323, 456  
Netzer, H. 1990, in *Active Galactic Nuclei: Saas-Fee Advanced Course 20*, ed. Courvoisier, T.J.-L. & Mayor, M. (Springer Verlag: Berlin), p. 57  
Peterson, B.M. 1994, in *Reverberation Mapping of the Broad-Line Region in Active Galactic Nuclei*, ed. Gondhalekar, P.M., Horne, K. & Peterson, B.M. (ASP Press: San Francisco), p. 1  
Rees, M., Netzer, H. & Ferland, G.J. 1989, *ApJ*, 347, 640  
Sun, W.H. & Malkan, M.A. 1991, *ApJ*, 346, 68  
Wandel, A. 1997, *ApJ*, 430, 131  
Wandel, A. & Boller, Th. 1998, *A&A*, 331, 884  
Wandel, A. & Liang, E. 1991, *ApJ*, 380, 84  
Wandel, A. & Mushotzky, R.F. 1986, *ApJ*, 306, L61  
Wandel, A. & Petrosian, V. 1988, *ApJ*, 329, L11  
Wandel, A. & Yahil, A. 1985, *ApJ*, 295, L1

Zheng, W., Kriss, G.A., Telfer, R.C., Grimes, J.P. & Davidsen, A.F. 1997, ApJ, 475, 469

## Discussion

*Brad Peterson:* I believe that a fairly reliable virial mass can be obtained from reverberation mapping data alone. The continuum emission-line cross-correlation function gives a centroid that measures the responsivity-weighted radius of the BLR. The spectra can be combined to form mean and rms spectra. The rms spectrum identifies the variable part of the emission line, and the line width used for virial estimates should be that measured from the rms spectrum. This way both the characteristic line width and scale size refer to the same gas, that which is varying at the time of the experiment.

*Amri Wandel:* I fully agree. This method actually gives “the best of both worlds”: a direct measurement of the distance along with the appropriately weighted velocity. It is interesting to compare the rms reverberation and the ionization-parameter methods, in order to calibrate the latter, which is used more readily and also for objects without variability data.

*Michael Corbin:* I wish to comment that there exists a strong correlation between the asymmetry of the C IV  $\lambda 1549$  and the H $\beta$  profiles and the luminosity of the soft X-ray and near UV continuum, such that as luminosity increases, the profiles become more red asymmetric. I have been able to model these redward asymmetries as the effect of gravitational redshift, which is proportional to the mass of the black hole. This correlation is therefore consistent with a universal black hole mass-luminosity relationship.

*Martin Gaskell:* It is interesting that the accretion disk method shows  $M$  tending to  $M_{\text{Edd}}$  when we go to high luminosities. From reverberation mapping (Koratkar & Gaskell 1991, ApJL) we found 3C273 near  $M_{\text{Edd}}$ . Prab Gondhalekar has found this to be generally true for high luminosity quasars. However, from our analyses of 3C273, I think that beaming of the continuum is causing an underestimate of the radius in reverberation mapping.

*Amri Wandel:* The trend of the  $L/M$  ratio to be larger for more luminous objects appears to be associated only with the accretion disk fitting method of mass estimation. When the mass is estimated by the ionization-parameter method, this trend is much weaker or even consistent with  $M \propto L$  (hence  $L/M \sim \text{const.}$ ). The correlation between  $L/M$  and the luminosity in the accretion disk method may therefore reflect a bias related to the thin accretion disk equations or the UV-X-ray continuum of AGN.

*Jean Clavel:* Observationally, how does one define a characteristic “fastest” X-ray variability? The power-density has a slope close to unity (e.g. is self-invariant), so that there is no characteristic time scale and the probability of observing an event of  $\Delta L$  within a time  $\Delta t$  increases with the length of the observation.

*Amri Wandel:* The variability time scale has been determined only from large events (change of the flux by a factor of 1.5 or more), and the characteristic time has then been taken as the e-folding time of that change.